
Adversarially-learned Inference via an Ensemble of Discrete Undirected Graphical Models

Adarsh K. Jeewajee
MIT CSAIL
jaks19@mit.edu

Leslie P. Kaelbling
MIT CSAIL
lpk@csail.mit.edu

Abstract

Undirected graphical models are compact representations of joint probability distributions over random variables. Given a distribution over inference tasks, graphical models of arbitrary topology can be trained using empirical risk minimization. However, when faced with new task distributions, these models (EGMs) often need to be re-trained. Instead, we propose an inference-agnostic adversarial training framework for producing an ensemble of graphical models (AGMs). The ensemble is optimized to generate data, and inference is learned as a by-product of this endeavor. AGMs perform comparably with EGMs on inference tasks that the latter were specifically optimized for. Most importantly, AGMs show significantly better generalization capabilities across distributions of inference tasks. AGMs are also on par with GibbsNet, a state-of-the-art deep neural architecture, which like AGMs, allows conditioning on any subset of random variables. Finally, AGMs allow fast data sampling, competitive with Gibbs sampling from EGMs.

1 Introduction

Probabilistic graphical models (Koller and Friedman, 2009; Murphy, 2012) are compact representations of joint probability distributions. We focus on *discrete pairwise undirected* graphical models, which represent the independence structure between pairs of random variables. Algorithms such as belief propagation allow for inference on these graphical models, with arbitrary choices of observed and hidden variables. When the graph topology is loopy, or when the structure is mis-specified, inference through belief propagation is approximate (Kulesza and Pereira, 2008).

A purely generative way to train such a model is to maximize the likelihood of some data, under the probability distribution induced by the model. This method is independent of any information about how we plan to use the model for inference. However, we are interested in conditional settings, where the model will be called upon to answer queries of the form

$$\hat{x}_Q = \arg \max_{x_Q} \mathbb{P}(X_Q = x_Q | X_{\mathcal{E}} = x_{\mathcal{E}}), \quad (1)$$

expressed in compact notation $(X_{\mathcal{E}} = x_{\mathcal{E}}, X_Q, X_{\mathcal{H}})$, where we observe random variables $X_{\mathcal{E}}$ and have to predict X_Q , with the possibility of some hidden variables $X_{\mathcal{H}}$ which have to be marginalized over, with \mathbb{P} representing the true data distribution. We note that observations $x_{\mathcal{E}}$ have to come from a data point from a given data distribution, and the values x_Q from that same data point are the ground truth values to be guessed. If we are given information about the distribution of queries the model will be called upon to answer, then we can improve its prediction performance, by shaping the query distribution used at parameter estimation time, accordingly. In degenerate query distributions, \mathcal{E} , Q and \mathcal{H} are fixed. When this is the case *and* \mathcal{H} is empty, we could use a Bayesian feed-forward neural network (Husmeier and Taylor, 1999) to model $\mathbb{P}(X_Q | X_{\mathcal{E}})$ and train it by backpropagation.

The *empirical risk minimization of graphical models* (EGM) framework of Stoyanov et al. (2011) and Domke (2013) generalizes this gradient-based parameter estimation idea to graphical models.

Their framework allows retaining any given graphical model structure, and back-propagating through a differentiable inference procedure to obtain model parameters that facilitate the query-evaluation problem. EGM allows solving the most general form of problems expressed as (1), where \mathcal{E} , \mathcal{Q} and \mathcal{H} are allowed to vary, essentially allowing a distribution over possible queries. Information about this distribution is used at training time to *sample* choices of evidence and query variable *indices* (\mathcal{E} , \mathcal{Q}), as well the *observed values* $x_{\mathcal{E}}$. They then train the whole imperfect system end-to-end through gradient propagation (Domke, 2010). This approach improves the inference accuracy on queries sampled from the training, by orders of magnitude compared to generative likelihood maximization.

One drawback of the EGM approach is that the training procedure is tailored to one specific distribution over inference tasks. To solve a very different inference task, the model would have to be completely re-trained. There also exist inference domains (as we see in section 4) where training on the task distribution that the model will eventually be tested on, is not the best choice, forcing practitioners to experiment in order to find the most informative training task distribution, given a known test task distribution.

Instead, we would like to learn discrete undirected graphical models which generalize over different or multi-modal task distributions, with little to no engineering. Our *adversarially trained graphical model* (AGM) strategy is built on the GAN framework (Goodfellow et al., 2014). It allows us to formulate a learning objective for our graphical models, aimed purely at optimizing the generation of samples from the model. No inference *task* distribution is needed for this learning approach. Our only assumption during training is that the training and testing *data sets* come from the same underlying distribution. Although our undirected graphical models need to be paired to a neural learner for the adversarial training, they are eventually detached from the learner, with an ensemble of parameterizations. When using one of the parameterizations, our graphical model is indistinguishable from one that was trained using alternative methods. We propose a mechanism for performing inference with the whole ensemble, which allows the desired generalization properties. Using an ensemble of models increases the expressive power of the final model, making up for approximations in inference and model mis-specification.

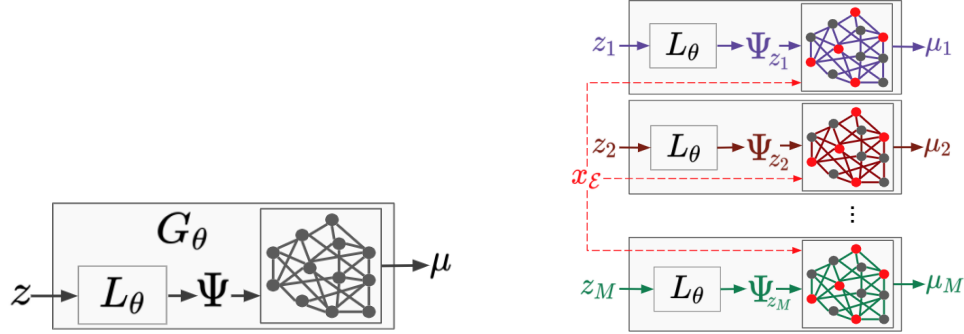
In the next sections, we discuss related work (2) and introduce our adversarial training framework (3) for undirected graphical models. Our first experiment (4.2), shows that although undirected graphical models with empirical risk minimization (EGMs) are trained specifically for certain inference tasks, our adversarially-trained graphical models (AGMs) can perform comparatively, despite having never seen those tasks prior to training. We also show that the AGM’s inference performance is on par with GibbsNet’s (Lamb et al., 2017), a deep adversarially trained inference network, despite using fewer parameters. The second experiment 4.3 showcases the generalization capabilities of AGMs across unseen inference tasks on images, and how EGMs’ knowledge does not translate to new tasks. In the last experiment 4.4, we show that the combination of AGMs and their neural learner provide a viable alternative for sampling from joint probability distributions in one shot, compared to Gibbs samplers defined on EGMs.

2 Related work

Our work combines *discrete, undirected* graphical models with the *GAN* framework for training. The graphical model is applied in *data space*, with the *belief propagation* algorithm used for *inference*, over an *ensemble of parameterizations*.

Combining an ensemble of models has been explored in classification (Bahler and Navarro, 2000) and unsupervised learning (Baruque, 2010). Combined models may each be optimized for a piece of the problem space (Jacobs et al., 1991) or may be competing on the same problem (Freund and Schapire, 1999). Linear and log-linear ensemble combinations like ours have been analyzed by Fumera and Roli (2005) and the closest work which uses the ensemble approach, by Antonucci et al. (2013), combines Bayesian networks for classification.

Using GANs to generate data from *discrete* distributions is an active area of research, including work of Fathony and Goela (2018), Dong and Yang (2018), and Camino et al. (2018), with applications in health (Choi et al., 2017) and quantum physics (Situ et al., 2018). Undirected graphical models have been embedded into neural pipelines before. For instance, Zheng et al. (2015) use them as RNNs, Ammar et al. (2014) and Johnson et al. (2016) use them in the neural autoencoder framework,



(a) **Training:** L_θ generates a vector of parameters Ψ from $z \sim \mathcal{N}(0, I_m)$ for the graphical model $G(V, E)$. Belief propagation generates the belief vector μ from Ψ . In the WGAN-GP scheme (see section 3.2), $\bar{x} := \mu$ is taken to be the fake data from generator G_θ , and is fed to discriminator D_w (not pictured).

(b) **Testing/Inference:** Given a query $(X_\mathcal{E} = x_\mathcal{E}, X_\mathcal{Q}, X_\mathcal{H})$, an ensemble of M graphical models parametrized by $\Psi_{z_1}, \dots, \Psi_{z_M}$ is produced by L_θ from $z_1, \dots, z_M \sim \mathcal{N}(0, I_m)$. Belief propagation on each model given the *same* observations $x_\mathcal{E}$ (red nodes) produces M conditional beliefs.

Figure 1: Our framework, during training (left) and as an ensemble during testing/inference (right).

Kuleshov and Ermon (2017) use them in neural variational inference pipelines, and Tompson et al. (2014) combine them with CNNs.

Other works use graph neural networks (Battaglia et al., 2018), but with some connection to classical undirected graphical models. For example, some works learn variants of, or improve on, message passing (Liu and Poulin, 2019; Satorras and Welling, 2020; Gilmer et al., 2017; Satorras et al., 2019). Other works combine classical graphical models and graph neural networks with one another (Qu et al., 2019), while some use neural networks to replace classical graphical model inference entirely (Yoon et al., 2018; Zhang et al., 2019).

Among the work closest to ours, Fathony et al. (2018) learn *tractable* graphical models using *exact inference* through adversarial objectives. Chongxuan et al. (2018) and Karaletsos (2016) use graphical models in adversarial training pipelines, but to model the posterior distribution. GANs have been used with graphs for high-dimensional representation learning (Wang et al., 2017), structure learning (Bojchevski et al., 2018) and classification (Zhong and Li, 2018). Other relevant GAN works focus on inference in the data space without the undirected graphical structure. For example the conditional GAN (Mirza and Osindero, 2014) and its variants (Xu et al., 2019) allow inference, but conditioned on variables specified during training. (Donahue et al., 2016) and (Dumoulin et al., 2017) introduced the idea of learning the reverse mapping from data space back to latent space in GANs. GibbsNet (Lamb et al., 2017) is the closest model to ours, though it is not graphical in the data space. GibbsNet allows inference conditioned on any subset of variables, like us. Their inference process is iterative as they transition from data space to latent space and back, *stochastically* several times, clamping observed values in the process. Our inference mechanism stays within data space, but is also iterative due to the belief propagation algorithm. Each model in our learned ensemble has significantly less parameters than GibbsNet.

3 Method

3.1 Preliminaries

We aim to learn the parameters for pairwise discrete undirected graphical models, adversarially. These models are structured as graphs $G(V, E)$, with each node in their node set V representing one variable in the joint probability distribution being modeled. The distribution is over variables $X_1^N := (X_1, \dots, X_N)$. For simplicity, we assume that all random variables can take on values from the same discrete set \mathcal{X} .

A graphical model carries a parameter vector Ψ . On each edge $(i, j) \in E$, there is one scalar $\psi_{i,j}$ for every pair of values (x_i, x_j) that the pair of connected random variables can admit. Therefore

every edge carries $|\mathcal{X}|^2$ parameters, and in all, the graphical model $G(V, E)$ carries $k = |E||\mathcal{X}|^2$ total parameters, all contained in the vector $\Psi \in \mathbb{R}^k$.

Through its parameter set Ψ , the model summarizes the joint probability distribution over the random variables up to a normalization constant \mathcal{Z} as:

$$q_{X_1^N}(x_1^N; \Psi) = \frac{1}{\mathcal{Z}} \prod_{(i,j) \in E} \psi_{ij}(x_i, x_j). \quad (2)$$

Instead of incrementally updating *one* set of parameters Ψ to train a graphical model $G(V, E)$, our method trains an uncountably infinite *ensemble* of graphical model parameters, adversarially. In our framework, our model admits a random vector $z \in \mathbb{R}^m$ sampled from a standard multivariate Gaussian as well as a deterministic transformation L_θ , from z to a graphical model parameter vector $\Psi_z = L_\theta(z) \in \mathbb{R}^k$, and where θ it to be trained. It also admits the deterministic transformation from Ψ_z to a joint probability distribution over random variables X_1^N , as given by function q in (2), which depends on the edge set E of the graph. Under our framework, the overall joint distribution over random variables X_1^N can be summarized as

$$p_{X_1^N}(x_1^N) = \int_{z \in \mathbb{R}^m} p_Z(z) p_{X_1^N|Z}(x_1^N|z) dz = \int_{z \in \mathbb{R}^m} p_Z(z) q_{X_1^N}(x_1^N; L_\theta(z)) dz \quad (3)$$

Through adversarial training, we will learn to map random vectors $z \in \mathbb{R}^m$ to data samples. The only learnable component of this mapping is the transformation of $z \in \mathbb{R}^m$ to $\Psi_z \in \mathbb{R}^k$ through L_θ . Given Ψ_z , the joint distribution $q_{X_1^N}(x_1^N; \Psi_z)$ is given in (2) and since the goal of adversarial training is to produce high-quality samples which are indistinguishable from real data, through the lens of some discriminator, the training process is priming each $\Psi_z = L_\theta(z)$ to specialize on a niche region of the domain of the true data distribution. From the point of view of Jacobs et al. (1991), we will have learnt ‘local experts’ Ψ_z , each specializing to a subset of the training distribution. The entire co-domain of L_θ is our ensemble of graphical models.

Finally, computing exact marginal probabilities using (2) is not possible as computing \mathcal{Z} is intractable. Hence, whenever we are given one vector Ψ_z from the ensemble of graphical model parameters, and some observations $x_\mathcal{E}$, we carry out a fixed number t of belief propagation iterations through the `inference`($x_\mathcal{E}, \Psi, t$) procedure, to obtain one conditional marginal probability distribution $\mu_{i|x_\mathcal{E}}$ for every $i \in V$ (The distributions $\mu_{i|x_\mathcal{E}}$ for $i \in \mathcal{E}$ are degenerate distributions with all probability mass on the observed value of random variable X_i). This `inference` procedure is one that we will re-use throughout our exposition, for learning (with $\mathcal{E} = \emptyset$) as well as for inference (with $\mathcal{E} \neq \emptyset$).

3.2 Adversarial training

Our adversarial training framework follows Goodfellow et al. (2014). The discriminator D_w is tasked with distinguishing between real and fake samples in data space. Our $(L_\theta, G(V, E))$ pair constitutes our generator G_θ as seen in figure 1a. Fake samples are produced by our generator G_θ , which as is standard, maps a given vector z sampled from a standard multivariate Gaussian distribution, to samples \tilde{x} .

One layer of abstraction deeper, the generative process G_θ is composed of L_θ is taking in random vector $z \in \mathbb{R}^m$ as input, and outputting a vector $v \in \mathbb{R}^k$. The graphical model receives v , runs `inference`($x_\mathcal{E} = \emptyset, \Psi = v, t = t'$), for a pre-determined t' , and outputs a set of marginal probability distributions μ_i for $i \in V$. Note that the set \mathcal{E} of observed variables is empty, since our training procedure is inference-agnostic.

In summary, the graphical model extends the computational process which generated v from z , with the deterministic recurrent process of belief propagation on its structure E . Note that a one-to-one correspondence from entries of v to graphical model parameters $\psi_{ij}(x_i, x_j)$ has to be pre-determined for L_θ and $G(V, E)$ to interface with one another.

Instead of categorical sampling from the beliefs μ_i to get a generated sample for the GAN training (Hjelm et al., 2017; Jang et al., 2017), we follow the WGAN-GP method (Gulrajani et al., 2017) for training our discrete GAN. In their formulation, the fake data point \tilde{x} is a concatenation of all the marginal probability distributions μ_i , in some specific order. This means that true samples from the

train data set have to be processed into a concatenation of the \mathcal{X} -dimensional one-hot encodings of the values they propose for every node, to similarly meet the input specifications of the discriminator.

We minimize the WGAN-GP objective (4) with the gradient $\nabla_{x'} \|D_w(x')\|_2$ penalized at points $x' = \epsilon x + (1 - \epsilon)\tilde{x}$ which lie on the line between real samples x and fake samples \tilde{x} . This regularizer is a tractable 1-Lipschitz enforcer on the discriminator function, which stabilizes the WGAN-GP training procedure.

$$\mathcal{L}(x, \tilde{x}) = \min_w \max_{\theta} \mathbb{E}_{\tilde{x} \sim \mathbb{Q}} [D_w(\tilde{x})] - \mathbb{E}_{x \sim \mathbb{P}} [D_w(x)] + \lambda \mathbb{E}_{x' \sim \mathbb{P}'} \left[(\nabla_{x'} \|D_w(x')\|_2 - 1)^2 \right]. \quad (4)$$

3.3 Inference using the ensemble of graphical models

Out of the various ways to coordinate responses from our ensemble of graphical model parameters (see section 2), we choose the log-linear pooling method of (Antonucci et al., 2013), for its simplicity.

Given a query of the form $(X_{\mathcal{E}} = x_{\mathcal{E}}, X_{\mathcal{Q}}, X_{\mathcal{H}})$ as seen in (1), we call upon a finite subset of our infinite ensemble of graphical models. We randomly sample $z_1, \dots, z_M \sim N(0, I_m)$ and map them to a collection of parameter vectors $(\Psi_{z_1} = L_{\theta}(z_1), \dots, \Psi_{z_M} = L_{\theta}(z_M))$. M sets of beliefs, for every node, are fetched through M parallel calls to the inference procedure: `inference` $(x_{\mathcal{E}}, \Psi = L_{\Theta}(z_j), t = t')$ for $j = 1, \dots, M$. The idea behind log-linear pooling is to aggregate the opinion of every model in our finite ensemble. Concretely, for every random variable X_i , its M obtained marginal distributions $\mu_{i|X_{\mathcal{E}}}(\cdot|x_{\mathcal{E}}; \Psi_{z_j})$ for $j = 1, \dots, M$ are aggregated as we show now, and in all our experiments, we used $M = 1000$:

$$\hat{x}_i = \arg \max_{x_i \in \mathcal{X}} \prod_{j=1}^M \mu_{i|X_{\mathcal{E}}}(x_i|x_{\mathcal{E}}; \Psi_{z_j})^{\frac{1}{M}}, \quad i = 1, \dots, N. \quad (5)$$

4 Experiments

4.1 Setup

For inference tasks of the type formulated in (1), we need strategies to create distributions over queries of the form: $(X_{\mathcal{E}} = x_{\mathcal{E}}, X_{\mathcal{Q}}, X_{\mathcal{H}})$. We note that queries need to be grounded in some data set of interest. In any query, observations $x_{\mathcal{E}}$ must come from a real data point from a data set of choice, and the original values of query variables are kept as targets for empirical risk objectives.

The query creation schemes used in our work are as follows, and we do not use hidden variables $X_{\mathcal{H}}$:

- (i) `fractional`(f): A fraction f of all variables are made into query variables, and the rest are revealed as evidence.
- (ii) `corrupt`(c): Every variable is independently switched, with probability c , to another value picked randomly from its discrete support. Then `fractional`(0.5) is applied to the data point to obtain the query as in (i).
- (iii) `window`(w): [Image only] The center square of width w pixels is hidden and those pixels become query variables, while the pixels around the square are revealed as evidence.
- (iv) `quadrant`(q): [Image only] One of the four quadrants of pixels is hidden, and those pixels become query variables. The other three quadrants are revealed as evidence.

Some instantiations of these schemes, with specific parameters, on image data, are shown in figure 2. We note that the train and test query creation policies do not have to match. In fact, experiment II is designed to test the failure points of AGMs and EGMs when this mismatch occurs.

Concerning data sets, we use: **ten binary data sets** used in previous probabilistic modelling work (example (Gens and Pedro, 2013)) spanning 16 to 1359 variables, and **two binary image data sets (28x28)** which are MNIST (LeCun and Cortes, 2010) with digits 0 to 9, and Caltech-101 Silhouettes (Li et al., 2004) with shape outlines from 101 different classes.

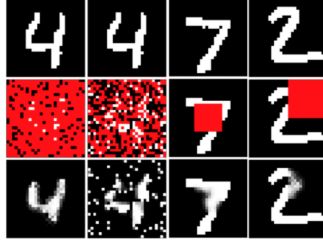


Figure 2: We have, in columns 1 to 4, the following query-creation schemes in action: `fractional(0.85)`, `corrupt(0.2)`, `window(10)` and `quadrant(1)`, respectively, as described in section 4.1. These schemes are applied to original MNIST images from row 1, to produce queries ($X_{\mathcal{E}} = x_{\mathcal{E}}, X_{\mathcal{Q}}, X_{\mathcal{H}}$) on row 2: visible original pixels are observations $X_{\mathcal{E}} = x_{\mathcal{E}}$, red pixels are $X_{\mathcal{Q}}$ to be guessed. Row 3 shows the marginals guessed by AGMs at every pixel (by plotting $\mathbb{P}(\text{pixel} = 1)$).

Table 1: Summary of data sets in columns 1-2, accuracies obtained in experiment I in columns 3-6 and accuracies from experiment III in columns 7-9. All values printed in this table are averaged over 3 runs.

| Name | $ \mathcal{V} $ | Experiment I | | | | Experiment III | | |
|-----------------------|-----------------|--------------|------|------------|----------|----------------|------------------------|-------------------------|
| | | EMP | EGM | AGM (ours) | GibbsNet | AGM sampler | Gibbs sampler (burn=0) | Gibbs sampler (burn=10) |
| NLTCS | 16 | 67.2 | 81.7 | 79.5 | 75.2 | 81.2 | 77.7 | 79.8 |
| Jester | 100 | 60.6 | 70.6 | 65.7 | 68.2 | 69.88 | 63.9 | 67.0 |
| Netflix | 100 | 52.1 | 66.0 | 63.9 | 69.5 | 64.7 | 61.4 | 61.8 |
| Accidents | 111 | 71.3 | 83.3 | 83.2 | 82.5 | 83.0 | 81.2 | 82.8 |
| Mushrooms | 112 | 81.2 | 88.0 | 87.3 | 87.2 | 86.8 | 85.3 | 86.1 |
| Adult | 123 | 88.7 | 92.1 | 92.1 | 91.9 | 92.0 | 90.6 | 91.9 |
| Connect 4 | 126 | 63.7 | 88.8 | 88.6 | 87.9 | 88.4 | 85.9 | 88.4 |
| Pumsb-star | 163 | 72.9 | 86.7 | 82.2 | 85.4 | 84.1 | 77.7 | 81.8 |
| 20 NewsGroup | 910 | 94.5 | 96.0 | 96.0 | 96.0 | 94.7 | 90.6 | 94.7 |
| Voting | 1359 | 65.8 | 99.8 | 92.4 | 90.6 | 94.8 | 67.6 | 64.1 |
| MNIST | 784 | 72.0 | 85.3 | 86.7 | 85.5 | 84.1 | 84.8 | 84.9 |
| MNIST (grid) | 784 | 89.0 | 93.8 | 94.5 | - | 93.0 | 91.0 | 92.8 |
| CALTECH | 784 | 56.0 | 74.8 | 77.8 | 78.3 | 69.0 | 68.4 | 68.4 |
| CALTECH (grid) | 784 | 82.9 | 93.2 | 94.4 | - | 92.2 | 92.0 | 92.1 |

4.2 Experiment I: Benchmarking

In this experiment, we train our models on each train data set separately, and test on 1000 unseen points. EMP is a baseline with edge parameters given by empirical probabilities. EGMs train by minimizing the conditional log likelihood score under the inference task given by `fractional(0.5)`. The query type (`fractional(0.7)`) is used to test every model. Accuracies are given in table 1 as the percentage of query variables correctly guessed, over all queries formed from the test set.

GibbsNet is the deep adversarially trained inference network introduced in section 2. Neural network architectures (AGM’s learner, GibbsNet) are given in the appendix. Graph methods (EMP, EGM and AGM) use randomized edge sets of size $\min(2000, 5|\mathcal{V}|)$. A grid structure is also separately tried, with image data, as seen in column 1 of table 1.

Results in table 1 show that while EGMs are explicitly trained on the `fractional(0.5)` task, AGMs are not far behind in performance in general, and are actually better on all image data sets. Perhaps a completely randomized graph is not the best choice with AGMs, although it did better than EGMs on image data with random graphs. Perhaps a future line of work would be to use AGMs in combination with structure-finding algorithms. GibbsNet being behind AGMs on both image data sets with grid graphs shows the usefulness of the relational inductive bias provided by the graph. GibbsNet is the best performer on image data when its competitors use randomized graphs, as it learns meaningful latent space representations that aid inference through its feed-forward architecture. However once AGMs are equipped with meaningful grid graphs, they get much higher scores on queries on images.

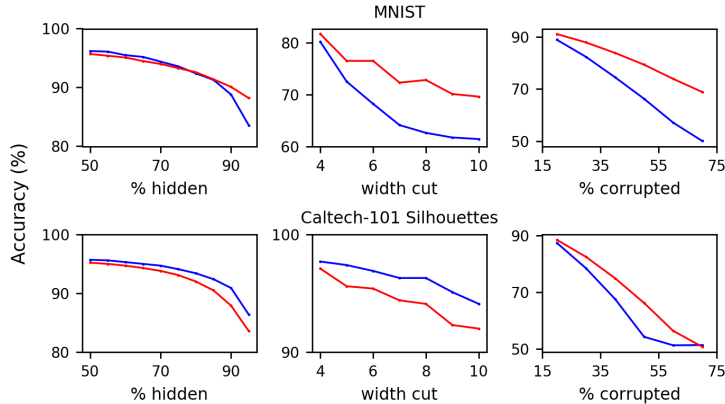


Figure 3: Some of the experiment II results: From left to right, results on `fractional` (0.5 to 0.95), `window` (4 to 10) and `corrupt` (0.2 to 0.7) queries, with the tasks getting more difficult as horizontal axis values go up. with MNIST (top) and Caltech-101 (bottom). AGM (ours) performances are in red, and EGMs trained on `fractional` (0.5), have their performances plotted in blue.

4.3 Experiment II: Generalization across inference tasks on images

In this experiment, we want to test how well AGMs and EGMs generalize across tasks of varying nature given that experiment 1 employed `fractional` tasks only. Can AGMs generalize to schemes like `corrupt`, `window` and `quadrant`, despite its inference-agnostic learning style? On the other hand, how widely applicable is an EGM trained using a particular query distribution?

- *One* AGM is trained adversarially, by definition. It will be evaluated on `fractional` (f), `corrupt` (c), `window` (w) and `quadrant` (q) tasks with parameter ranges $f = 0.5$ to 0.95, $c = 0.2$ to 0.7 $w = 4$ to 10 respectively.
- *Multiple* EGMs are trained separately on `fractional` (0.5), `corrupt` (0.5), `window` (7) and `quadrant` (1) tasks, and evaluated for each resulting model on the same test suite used to test AGMs.
- *One* mixture EGM (named MIX in table 2) is trained by sampling queries successively from the tasks mentioned in the last bullet.

Results are reported through figure 3 and table 2. Figure 3 plots performance of AGM, and that of EGM trained on `fractional` (0.5) which was the non-mixture EGM which generalized best to other tasks, as corroborated by table 2. Figure 3 shows that AGMs learn to perform well across tasks and are more robust to extreme versions of the tasks as performance does not degrade catastrophically as we move to higher x-axis task parameters. The decay is generally steeper for EGMs.

Table 2 shows performance of EGMs trained on query distributions shown in the first column, and tested on query distributions, spread horizontally. Looking at the first four rows (EGMs only), the highest value is mostly on the diagonal as expected when train and test query distributions match, for both MNIST and Caltech-101 but the second-highest is always EGM trained on `fractional` (0.5). Adding in the row for AGMs, we now see that AGMs are even closer to the highest EGM score in every column, showing the best generalization, despite having never explicitly learned to infer, and never having seen these task domains. The mean score (last column per data set) indicates this as well. Lastly, we introduce the last row, with MIX as described above, and MIX comes closest to AGMs. Better performances between the two are indicated by a grey shaded table cell. But even after every possible test task information was baked into the training procedure of MIX, it surpasses AGMs only in three out of 8 tasks, and has a lower mean score.

An interesting result is that neither training on `window` (7) itself, nor on a mixture as MIX did, constitutes the best way to prepare a model to be tested on `window` (7) queries, in the Caltech-101 case. This corroborates the idea that it is not always immediately clear, which training task distribution should be picked for testing on a given test task distribution as discussed in section 1.

Table 2: Cross-task results (averaged over 3 trials) for EGMs (first 4 rows), AGM and MIX (an EGM trained on a mixture of tasks). Means of the rows indicate relative generalization abilities

| | MNIST | | | | | Caltech-101 Silhouettes | | | | |
|--------------|-------------|-------------|-------------|-------------|-------------|-------------------------|-------------|-------------|-------------|-------------|
| | f=0.5 | w=7 | c=0.5 | q=1 | mean | f=0.5 | w=7 | c=0.5 | q=1 | mean |
| f=0.5 | 96.2 | 64.1 | 66.3 | 84.1 | 77.7 | 95.7 | 96.3 | 54.3 | 80.0 | 81.6 |
| w=7 | 53.4 | 73.4 | 51.0 | 49.0 | 56.7 | 55.0 | 96.0 | 52.0 | 52.7 | 63.9 |
| c=0.5 | 85.1 | 57.2 | 84.5 | 83.9 | 77.7 | 76.7 | 88.6 | 77.1 | 76.4 | 79.7 |
| q=1 | 60.6 | 53.8 | 56.8 | 87.7 | 64.7 | 60.6 | 64.5 | 54.0 | 82.5 | 65.4 |
| AGM | 95.7 | 72.3 | 79.2 | 87.4 | 83.7 | 95.2 | 94.2 | 66.2 | 80.1 | 83.9 |
| MIX | 93.7 | 66.9 | 82.4 | 86.8 | 82.5 | 92.0 | 90.0 | 70.2 | 80.6 | 83.2 |

4.4 Experiment III: Sampling using AGMs instead of Gibbs sampling

Motivated by the crisp image samples generated from AGMs and smooth interpolation in latent space (see appendix) (which is an interesting result, given that CNNs were not included in our discrete GAN architecture), we decided to compare sample quality from AGMs versus from Gibbs samplers defined on EGMs.

We would like some metric for measuring sample quality and quantifying the generative ability of our models. We design the following test, which in a way measures, whether the samplers could generate data to teach a new model to solve an inference task, from scratch.

We train an AGM and an EGM on some training data set A. We generate 1000 samples from each model, and call these sampled data sets S_1 and S_2 . If we now train a freshly-created EGM E_1 on S_1 and another one, E_2 , on S_2 , from scratch, (call these EGMs evaluators) then test them on the true test data set of A, then which one out of E_1 or E_2 has better performance, assuming everything else about them is identical? If E_1 performs better, then data from the AGM was of better quality, or vice versa. Note that to train and test all EGMs in this experiment (including the one that was eventually used for sampling), the query type was fixed as `fractional(0.5)`.

For the Gibbs sampler defined on the EGM, we try two scenarios: one where it uses no burn-in cycles to be similar to the one-shot sampling procedure of an AGM (one-shot meaning one pass from z to Ψ to x), and one scenario where it has 10 burn-in cycles.

Interestingly, as seen in table 1, the AGM sampler is better than the Gibbs sampler regardless of the number of burn-in cycles, bar one exception, and performance when trained on AGM samples is not that far off the performance from real training data. For the Gibbs sampler, even 10 burn-in steps are not enough for the Markov chain being sampled from to mix. Since variables have to be sequentially sampled in the Gibbs sampler, it takes orders of magnitude more time to sample from it, compare to sampling from an AGM. The bottleneck in run-time for the AGM is the belief propagation algorithm, but it is parallelizable across edges and can be run entirely using matrix operations (Bixler and Huang, 2018). Hence sampling from the AGM is a viable solution, when samples of good quality are needed in the least possible time.

5 Conclusion

The common approach for training undirected graphical models when the test inference task distribution is known already, is empirical risk minimization. In this work, we showed the weaknesses of models (EGMs) produced using this approach. They fail to generalize across task distributions, and they do not necessarily scale to harder versions of the tasks they were trained on. We introduced an adversarial training framework for undirected graphical models, which instead of producing one model, learns a whole ensemble of models. Learning an ensemble increases the expressive power of the final model, making up for approximations in inference and model mis-specification. As shown in our experiments, our models (AGMs) were able to generalize over an array of inference task distributions, even outperforming an EGM that was trained on the whole mixture of test inference tasks that we used. We also showed that AGMs perform comparably with GibbsNet, which is a deep adversarially learned model for inference. Finally, we showed glimpses of the generative

abilities of AGMs, when coupled with their neural learner modules. Notably, AGMs can sample data in one fast pass through the model and is a more efficient and accurate sampler than a Gibbs sampler defined on an EGM.

References

- Waleed Ammar, Chris Dyer, and Noah A. Smith. Conditional random field autoencoders for unsupervised structured prediction. *CoRR*, abs/1411.1147, 2014. URL <http://arxiv.org/abs/1411.1147>.
- Alessandro Antonucci, Giorgio Corani, Denis Deratani Mauá, and Sandra Gabaglio. An ensemble of bayesian networks for multilabel classification. In *Twenty-Third International Joint Conference on Artificial Intelligence*, 2013.
- Dennis Bahler and Laura Navarro. Methods for combining heterogeneous sets of classifiers, 2000.
- B. Baruque. *Fusion Methods for Unsupervised Learning Ensembles*. Studies in Computational Intelligence. Springer Berlin Heidelberg, 2010. ISBN 9783642162046. URL <https://books.google.com/books?id=oVGnmPT0I48C>.
- Peter W. Battaglia, Jessica B. Hamrick, Victor Bapst, Alvaro Sanchez-Gonzalez, Vinícius Flores Zambaldi, Mateusz Malinowski, Andrea Tacchetti, David Raposo, Adam Santoro, Ryan Faulkner, Çaglar Gülçehre, H. Francis Song, Andrew J. Ballard, Justin Gilmer, George E. Dahl, Ashish Vaswani, Kelsey R. Allen, Charles Nash, Victoria Langston, Chris Dyer, Nicolas Heess, Daan Wierstra, Pushmeet Kohli, Matthew Botvinick, Oriol Vinyals, Yujia Li, and Razvan Pascanu. Relational inductive biases, deep learning, and graph networks. *CoRR*, abs/1806.01261, 2018. URL <http://arxiv.org/abs/1806.01261>.
- Reid Bixler and Bert Huang. Sparse-matrix belief propagation. In *UAI*, 2018.
- Aleksandar Bojchevski, Oleksandr Shchur, Daniel Zügner, and Stephan Günnemann. Netgan: Generating graphs via random walks. In *ICML*, 2018.
- Ramiro Camino, Christian A. Hammerschmidt, and Radu State. Generating multi-categorical samples with generative adversarial networks. *ArXiv*, abs/1807.01202, 2018.
- Edward Choi, Siddharth Biswal, Bradley Malin, Jon Duke, Walter F. Stewart, and Jimeng Sun. Generating multi-label discrete patient records using generative adversarial networks. In *MLHC*, 2017.
- LI Chongxuan, Max Welling, Jun Zhu, and Bo Zhang. Graphical generative adversarial networks. In *Advances in neural information processing systems*, pages 6069–6080, 2018.
- J. Domke. Learning graphical model parameters with approximate marginal inference. *IEEE Transactions on Pattern Analysis and Machine Intelligence*, 35(10):2454–2467, 2013.
- Justin Domke. Implicit differentiation by perturbation. In J. D. Lafferty, C. K. I. Williams, J. Shawe-Taylor, R. S. Zemel, and A. Culotta, editors, *Advances in Neural Information Processing Systems 23*, pages 523–531. Curran Associates, Inc., 2010. URL <http://papers.nips.cc/paper/4107-implicit-differentiation-by-perturbation.pdf>.
- Jeff Donahue, Philipp Krähenbühl, and Trevor Darrell. Adversarial feature learning. *CoRR*, abs/1605.09782, 2016. URL <http://arxiv.org/abs/1605.09782>.
- Hao-Wen Dong and Yi-Hsuan Yang. Training generative adversarial networks with binary neurons by end-to-end backpropagation. *CoRR*, abs/1810.04714, 2018. URL <http://arxiv.org/abs/1810.04714>.
- Vincent Dumoulin, Ishmael Belghazi, Ben Poole, Alex Lamb, Martín Arjovsky, Olivier Mastropietro, and Aaron C. Courville. Adversarially learned inference. *ArXiv*, abs/1606.00704, 2017.
- Rizal Fathony and Naveen Goela. Discrete wasserstein generative adversarial networks (dwgan). 2018.

- Rizal Fathony, Ashkan Rezaei, Mohammad Ali Bashiri, Xinhua Zhang, and Brian Ziebart. Distributionally robust graphical models. In S. Bengio, H. Wallach, H. Larochelle, K. Grauman, N. Cesa-Bianchi, and R. Garnett, editors, *Advances in Neural Information Processing Systems 31*, pages 8344–8355. Curran Associates, Inc., 2018. URL <http://papers.nips.cc/paper/8055-distributionally-robust-graphical-models.pdf>.
- Yoav Freund and Robert Schapire. A short introduction to boosting. *Journal-Japanese Society For Artificial Intelligence*, 14(771-780):1612, 1999.
- G. Fumera and F. Roli. A theoretical and experimental analysis of linear combiners for multiple classifier systems. *IEEE Transactions on Pattern Analysis and Machine Intelligence*, 27(6): 942–956, 2005.
- Robert Gens and Domingos Pedro. Learning the structure of sum-product networks. In Sanjoy Dasgupta and David McAllester, editors, *Proceedings of the 30th International Conference on Machine Learning*, volume 28 of *Proceedings of Machine Learning Research*, pages 873–880, Atlanta, Georgia, USA, 17–19 Jun 2013. PMLR. URL <http://proceedings.mlr.press/v28/gens13.html>.
- Justin Gilmer, Samuel S. Schoenholz, Patrick F. Riley, Oriol Vinyals, and George E. Dahl. Neural message passing for quantum chemistry. *CoRR*, abs/1704.01212, 2017. URL <http://arxiv.org/abs/1704.01212>.
- Ian J. Goodfellow, Jean Pouget-Abadie, Mehdi Mirza, Bing Xu, David Warde-Farley, Sherjil Ozair, Aaron C. Courville, and Yoshua Bengio. Generative adversarial networks. *ArXiv*, abs/1406.2661, 2014.
- Ishaan Gulrajani, Faruk Ahmed, Martín Arjovsky, Vincent Dumoulin, and Aaron C. Courville. Improved training of wasserstein gans. *ArXiv*, abs/1704.00028, 2017.
- R. Devon Hjelm, Athul Paul Jacob, Tong Che, Kyunghyun Cho, and Yoshua Bengio. Boundary-seeking generative adversarial networks. *ArXiv*, abs/1702.08431, 2017.
- Dirk Husmeier and J. G. Taylor. *Neural Networks for Conditional Probability Estimation: Forecasting beyond Point Predictions*. Springer-Verlag, Berlin, Heidelberg, 1st edition, 1999. ISBN 1852330953.
- Robert A Jacobs, Michael I Jordan, Steven J Nowlan, and Geoffrey E Hinton. Adaptive mixtures of local experts. *Neural computation*, 3(1):79–87, 1991.
- Eric Jang, Shixiang Gu, and Ben Poole. Categorical reparameterization with gumbel-softmax. *ArXiv*, abs/1611.01144, 2017.
- Matthew J. Johnson, David Duvenaud, Alexander B. Wiltschko, Ryan P. Adams, and Sandeep Robert Datta. Composing graphical models with neural networks for structured representations and fast inference. In *NIPS*, 2016.
- Theofanis Karaletsos. Adversarial message passing for graphical models. *ArXiv*, abs/1612.05048, 2016.
- Daphne Koller and Nir Friedman. *Probabilistic Graphical Models: Principles and Techniques - Adaptive Computation and Machine Learning*. The MIT Press, 2009. ISBN 0262013193.
- Volodymyr Kuleshov and Stefano Ermon. Neural variational inference and learning in undirected graphical models. *CoRR*, abs/1711.02679, 2017. URL <http://arxiv.org/abs/1711.02679>.
- Alex Kulesza and Fernando Pereira. Structured learning with approximate inference. In *Advances in Neural Information Processing Systems 20*. Cambridge, MA, 2008. URL http://books.nips.cc/papers/files/nips20/NIPS2007_0809.pdf.
- Alex Lamb, R. Devon Hjelm, Yaroslav Ganin, Joseph Paul Cohen, Aaron C. Courville, and Yoshua Bengio. Gibbsnet: Iterative adversarial inference for deep graphical models. In *NIPS*, 2017.
- Yann LeCun and Corinna Cortes. MNIST handwritten digit database. 2010. URL <http://yann.lecun.com/exdb/mnist/>.

- Fei-Fei Li, Rob Fergus, and Pietro Perona. Learning generative visual models from few training examples: An incremental bayesian approach tested on 101 object categories. *2004 Conference on Computer Vision and Pattern Recognition Workshop*, pages 178–178, 2004.
- Ye-Hua Liu and David Poulin. Neural belief-propagation decoders for quantum error-correcting codes. *Physical review letters*, 122 20:200501, 2019.
- Mehdi Mirza and Simon Osindero. Conditional generative adversarial nets. *CoRR*, abs/1411.1784, 2014. URL <http://arxiv.org/abs/1411.1784>.
- Kevin P. Murphy. *Machine Learning: A Probabilistic Perspective*. The MIT Press, 2012. ISBN 0262018020.
- Meng Qu, Yoshua Bengio, and Jian Tang. Gmnn: Graph markov neural networks. In *ICML*, 2019.
- Victor Garcia Satorras and M. Welling. Neural enhanced belief propagation on factor graphs. *ArXiv*, abs/2003.01998, 2020.
- Victor Garcia Satorras, Zeynep Akata, and M. Welling. Combining generative and discriminative models for hybrid inference. *ArXiv*, abs/1906.02547, 2019.
- Haozhen Situ, Zhi-Min He, Lvzhou Li, and Shenggen Zheng. Quantum generative adversarial network for generating discrete data. 2018.
- Veselin Stoyanov, Alexander Ropson, and Jason Eisner. Empirical risk minimization of graphical model parameters given approximate inference, decoding, and model structure. In Geoffrey Gordon, David Dunson, and Miroslav Dudík, editors, *Proceedings of the Fourteenth International Conference on Artificial Intelligence and Statistics*, volume 15 of *Proceedings of Machine Learning Research*, pages 725–733, Fort Lauderdale, FL, USA, 11–13 Apr 2011. PMLR. URL <http://proceedings.mlr.press/v15/stoyanov11a.html>.
- Jonathan Tompson, Arjun Jain, Yann LeCun, and Christoph Bregler. Joint training of a convolutional network and a graphical model for human pose estimation. *CoRR*, abs/1406.2984, 2014. URL <http://arxiv.org/abs/1406.2984>.
- Hongwei Wang, Jia Wang, Jialin Wang, Miao Zhao, Weinan Zhang, Fuzheng Zhang, Xing Xie, and Minyi Guo. Graphgan: Graph representation learning with generative adversarial nets. *CoRR*, abs/1711.08267, 2017. URL <http://arxiv.org/abs/1711.08267>.
- Lei Xu, Maria Skoularidou, Alfredo Cuesta-Infante, and Kalyan Veeramachaneni. Modeling tabular data using conditional GAN. *CoRR*, abs/1907.00503, 2019. URL <http://arxiv.org/abs/1907.00503>.
- KiJung Yoon, Renjie Liao, Yuwen Xiong, Lisa Zhang, Ethan Fetaya, Raquel Urtasun, Richard S. Zemel, and Xaq Pitkow. Inference in probabilistic graphical models by graph neural networks. *CoRR*, abs/1803.07710, 2018. URL <http://arxiv.org/abs/1803.07710>.
- Zhen Zhang, Fan Wu, and Wee Sun Lee. Factor graph neural network. *CoRR*, abs/1906.00554, 2019. URL <http://arxiv.org/abs/1906.00554>.
- Shuai Zheng, Sadeep Jayasumana, Bernardino Romera-Paredes, Vibhav Vineet, Zhizhong Su, Dalong Du, Chang Huang, and Philip H. S. Torr. Conditional random fields as recurrent neural networks. *CoRR*, abs/1502.03240, 2015. URL <http://arxiv.org/abs/1502.03240>.
- Zilong Zhong and Jonathan Li. Generative adversarial networks and probabilistic graph models for hyperspectral image classification. *CoRR*, abs/1802.03495, 2018. URL <http://arxiv.org/abs/1802.03495>.